

A DAMPING RING DESIGN FOR FUTURE LINEAR COLLIDERS

T. O. RAUBENHEIMER, W. E. GABELLA, P. L. MORTON, M. J. LEE, L. Z. RIVKIN, R. D. RUTH

Stanford Linear Accelerator Center, Stanford University, Stanford, CA, 94309

ABSTRACT

In this paper we present a preliminary design of a damping ring for the TeV Linear Collider (TLC), a future linear collider with an energy of 1/2 to 1 TeV in the center of mass.¹ Because of limits on the emittance, repetition rate and longitudinal impedance, we use combined function FODO cells with wigglers in insertion regions; there are approximately 22 meters of wigglers in the 155 meter ring. The ring has a normalized horizontal emittance, including the effect of intrabeam scattering, which is less than 3×10^{-6} and an emittance ratio of $\epsilon_x \approx 100\epsilon_y$. It is designed to damp bunches for 7 vertical damping times while operating at a repetition rate of 360 Hz. Because of these requirements on the emittance and the damping per bunch, the ring operates at 1.8 GeV and is relatively large, allowing more bunches to be damped at once.

INTRODUCTION

The basic design goals of the TLC damping ring are compared with those of the Stanford Linear Collider (SLC) damping rings in Table 1. The emittances listed in Table 1 are the extracted beam emittances when running at the specified repetition rate. In addition, the SLC parameters listed assume that the rings are coupled by running on the difference resonance. Although we have measured 50:1 equilibrium emittance ratios when the SLC rings are uncoupled, the rings cannot achieve such large emittance ratios when operating at the full repetition rate, since they are limited by the damping requirements.

Table 1. Basic parameters of the SLC and TLC damping rings.

	TLC	SLC
Energy	1 ~ 2 GeV	1.15 GeV
Emittance, $\gamma\epsilon_x$	3.0 μmrad	26. μmrad ³
Emittance, $\gamma\epsilon_y$	30. nmrad	26. μmrad
Repetition rate	360 Hz	180 Hz
Bunch length	4 mm	5 mm ⁴

Thus the vertical emittance in the TLC must be damped to a value three orders of magnitude smaller than the SLC emittance. In addition, the repetition rate of the TLC ring has doubled. Thus the TLC ring will either have much faster damping times than the SLC ring or be much larger, thereby damping more bunches at once. In addition, the desired longitudinal emittance of the TLC ring is similar to that of the SLC. Since the transverse emittances are significantly smaller, this implies that intrabeam scattering and coherent effects will be important in the TLC design.

In the next section we will describe the basic lattice of the ring and list the main parameters. We will then discuss the wig-

glers used in the design and possible improvements and modifications. Finally, we will describe the chromatic correction scheme and the resulting dynamic aperture. Due to space limitations, the description of the design must be brief. In particular, we will not discuss collective effects although they impose severe constraints and thereby strongly influence the design. In addition, we will not discuss the tolerances required to achieve the desired 100:1 emittance ratio. The design is described in greater detail in Ref. 2. Reference 2 also contains a discussion of the constraints and the scaling process that led to the design

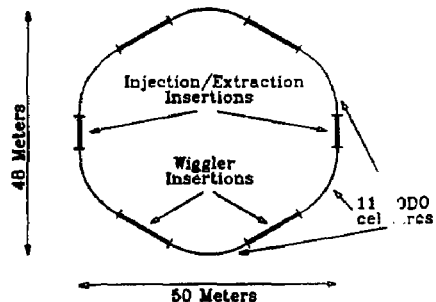


Fig. 1. Schematic of the TLC damping ring.

Table 2. TLC damping ring parameters.

Energy	$E_0 = 1.8 \text{ GeV}$
Length	$L = 155.1 \text{ m}$
Lattice	FODO with 22 meters of wiggler
Tunes	$\nu_x = 24.37 \quad \nu_y = 11.27$
Momentum compaction	$\alpha = 0.00120$
Design Current	10 batches of 10 bunches of $2 \times 10^{10} e^+ / e^-$

BASIC LATTICE

A design for the TLC damping ring is illustrated in Fig. 1. The ring has a circumference of 155 m and operates at an energy of 1.8 GeV. There are six insertion regions, two for injection/extraction and four for wigglers. The arcs between each insertion region are composed of 11 combined function FODO cells. The ring has a superperiodicity of two. The parameters are listed in Tables 2, 3, and 4. Table 2 lists general parameters while Tables 3 and 4 list transverse and longitudinal parameters with the wigglers on and off. The extracted emittances, listed in Table 3, are calculated assuming injected beam emittances of $\gamma\epsilon_x = 3 \times 10^{-6}$ mrad. Finally, the optical functions β_x and β_y and the dispersion function η_x for half of the ring are plotted in Fig. 2.

¹ Work supported by the Department of Energy, contract, DE-AC03-76SF00515

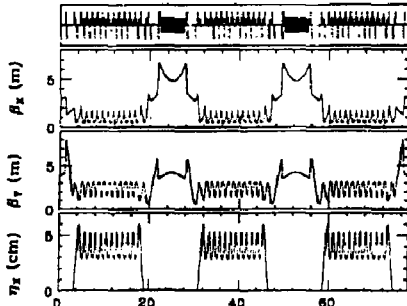


Fig. 2. Optical functions for half of the ring.

Table 3. TLC damping ring transverse parameters.

	Wigglers Off	Wigglers On
Natural emittance $\gamma\epsilon_x$	2.46 μmrad	2.00 μmrad
$\gamma\epsilon_x$ at design current	3.33 μmrad	2.74 μmrad
Damping τ_x	3.88 ms	2.50 ms
Damping τ_y	9.19 ms	3.98 ms
Damp. partition J_x	2.37	1.59
Rep. rate f_{rep}	155 Hz	360 Hz
Extracted $\gamma\epsilon_x$	3.33 μmrad	2.74 μmrad
Extracted $\gamma\epsilon_y$	0.035 μmrad	0.029 μmrad
Natural chrom. ξ_x	-28.35	-26.07
Natural chrom. ξ_y	-25.10	-22.27

The ring would operate with 10 batches of 10 bunches of 2×10^{10} electrons/positrons. The bunches in a batch are separated by 1 RF period, approximately 20 cm. Each batch is then separated by 50 ns, leaving 100 ns for the kicker pulse to rise and fall. In addition, since the bunches in a batch are closely spaced, the ring will need to use specially designed RF cavities to avoid multi-bunch instabilities: this is discussed in Ref. 5. Finally, the ring must have small longitudinal and transverse impedances to avoid the single bunch microwave instability and the mode coupling instability. The longitudinal microwave threshold occurs at the design current of $N = 2 \times 10^{10} e^+ / e^-$ when the effective longitudinal impedance is $(Z/n)_\parallel = 0.2 \Omega$. We hope to achieve this low value by using a smooth beam pipe, 1 cm in radius.

When the wigglers are on, the normalized horizontal emittance, including the intrabeam scattering effects calculated by ZAP,⁶ is 2.74×10^{-6} mrad. Because the ring operates at a relatively high energy, the intrabeam scattering contribution to the emittance is fairly small — about 27% of the ring emittance. The damping times, with the wigglers on, are $\tau_x = 2.50$ ms and $\tau_y = 3.98$ ms. This allows each batch to remain in the ring for seven vertical damping times when operating at a repetition rate of 360 Hz. Ignoring coupling of the horizontal and vertical planes, 7 vertical damping times will damp a positron beam with an initial normalized emittance of 3×10^{-3} to an emittance of 2.7×10^{-9} mrad. Thus to satisfy the vertical emittance requirement of 3×10^{-8} , the equilibrium vertical emittance must be less than 2.7×10^{-6} mrad. The alignment tolerances required to achieve this small vertical emittance are discussed in Refs. 2 and 7.

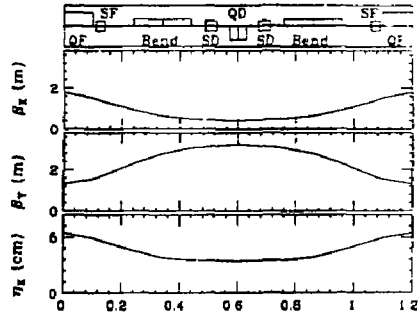


Fig. 3. Arc cell optics and magnets.

Table 4. TLC damping ring longitudinal parameters.

	Wigglers Off	Wigglers On
Radiation/turn U_0	203 KeV	466 KeV
Energy spread σ_e	0.00126	0.00104
Bunch length σ_z	5.5 mm	4.6 mm
RF frequency f_{RF}	1.4 GHz	1.4 GHz
RF voltage V_{RF}	.75 MV	.75 MV
Synch. tune ν_s	0.0068	0.0068

The six arcs are constructed of 11 combined function FODO cells. The bends have an additional defocusing quadrupole gradient which re-partitions the damping. The optical functions and the magnet positions are plotted for a single cell in Fig. 3. The bending magnets bend an angle of 2.5° and have normalized defocusing gradients of $K_1 = 5.0 \text{ m}^{-2}$, i.e. a gradient of 300 KG/meter. The QF's, the focusing quadrupoles, which are the strongest quadrupoles in the ring, have normalized gradients of -15.7 m^{-2} . Assuming a magnetic radius of $r = 1.2 \text{ cm}$, 2mm greater than the beam pipe, the QF's have pole tip fields of 11.3 KG.

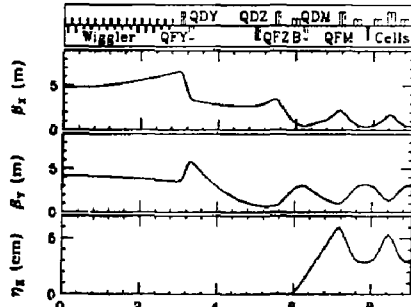


Fig. 4. Half of the wiggler insertion with wigglers on.

The six insertion regions are similar. The injection/extraction regions have a 2 m drift space for the septum magnets and the wiggler insertion regions have 6 m drift spaces. All six of the insertions contain dispersion suppression sections. Zero dispersion in the injection/extraction regions makes matching to the transport lines simpler, and zero dispersion in the wiggler insertions prevents the wigglers from increasing the emittance. In addition, the wiggler insertion regions have four independent

quadrupoles so the wiggler field can be varied while keeping the phase advance across the region constant. Finally, the lattice functions for half of a wiggler insertion region are plotted in Fig 4. Notice that the vertical focusing due to the wigglers allows β_y to have negative curvature across the insertion.

WIGGLERS

Wigglers are required to reduce the damping times by a factor of approximately 2.5. Thus, high peak fields are needed. Unfortunately, to prevent the wigglers from blowing up the emittance, short wiggler periods are also necessary. We are considering either strong hybrid wigglers $B_w \gtrsim 20\text{KG}$ or superconducting wigglers $B_w \gtrsim 40\text{KG}$. Strong wigglers are desirable since the required length of wiggler scales as $1/B_w^2$. Unfortunately, the non-linear effects scale with the wiggler strength and period as $L_w B_w^2 / \lambda_w^2$.⁶ Furthermore, the wiggler period scales as $\lambda_w^2 \sim 1/B_w^2$. Thus the non-linear terms would appear increase as strength cubed.

At this time we have not studied the non-linear effects and issues such as cost, practicality, etc., in detail. For this design we chose a wiggler with a 24 KG peak field, a filling factor of 50%, and a period of 20 cm. To meet the damping time requirement we need 22.4 meters of this wiggler. The period and the peak field were chosen to be within 15%¹⁰ of the limits for Nd-Fe-B hybrid wigglers as specified in Ref 9. If such high peak fields are not feasible, we can increase the energy of the design to 1.9 GeV and decrease the peak wiggler fields to 21 KG. The vertical damping time remains 3.98 ms and the natural horizontal normalized emittance increases to $2.29 \times 10^{-6}\text{mrad}$; intrabeam scattering further increases this to $2.85 \times 10^{-6}\text{mrad}$. The small increase in emittance occurs because the horizontal damping partition J_x increases as the wiggler gets weaker. Finally, we should mention that it is possible to design a ring without wigglers, but the ring would have to be larger and the operating energy would be $\sim 3\text{GeV}$.

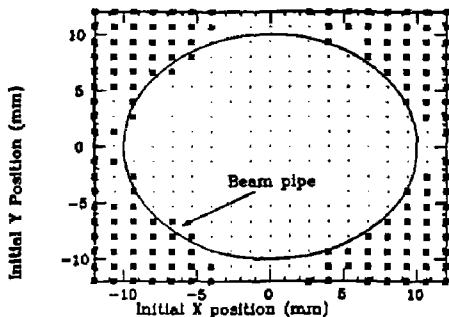


Fig. 5. Dynamic aperture for the chromatically corrected ring.

CHROMATIC CORRECTION

Before attempting to optimize the ring, we need to demonstrate that the chromatically corrected ring can have reasonable dynamic aperture. We currently correct the chromaticity with only two families of sextupoles located in the arcs. The integrated sextupole strengths are: $K_{2SF} = -52.0\text{m}^{-2}$ and $K_{1SD} = 68.7\text{m}^{-2}$. While there is more space between magnets in this design than in the SLC damping rings, the cells are still tightly packed. Thus we plan to use permanent magnet sextupoles similar to those successfully used in the SLC rings.

The phase advance of the cells is adjusted to nearly cancel the first order geometrics over an arc of 11 cells. We chose cell phase advances of $\nu_{xc} = .270$ and $\nu_{yc} = .086$. Thus

$$\begin{aligned} 11\nu_{xc} &\approx 3 & 11(3\nu_{xc}) &\approx 9 \\ 11(\nu_{xc} + 2\nu_{yc}) &\approx 5 & 11(\nu_{xc} - 2\nu_{yc}) &\approx 1. \end{aligned}$$

While this choice of phase advance cancels the first order geometrics over an arc, it drives the octupole difference resonance, a higher order geometric effect of sextupoles. Although we have not tried, we should be able to minimize the higher order geometric and higher order chromatic effects with additional sextupole families.

We have not attempted any optimization other than adjusting the cell phase advances as described above. The dynamic aperture is, for the most part, larger than the physical aperture. The results of tracking 1000 turns are plotted in Fig 5. Note that the plot is distorted; the beam pipe is round. The dynamic aperture will decrease when errors and realistic wiggler induced non-linear fields are included, however, with more sophisticated chromatic correction schemes we hope to be able to recover the good dynamic aperture.

SUMMARY

In this paper we present a design for a damping ring for a TeV linear collider. The ring is based upon a FODO lattice where the bending magnets contain a gradient to re-partition the damping. In addition, damping wigglers are used to lower the operating energy and to increase the energy spread, thereby increasing the threshold of the coherent instabilities.

We demonstrate, using a very simple chromatic correction scheme, that the chromatically corrected ring has reasonable dynamic aperture. We have not yet calculated the effect of alignment errors on the dynamic aperture and we have not included realistic non-linear wiggler fields. We believe that loss in dynamic aperture due to these effects can be recovered using additional families of sextupoles.

Finally, we note that we need to study the choice of wiggler in greater detail. In addition, we should take detailed looks at designs based upon lattices other than the FODO structure.

REFERENCES

1. See references in: *Proceedings of the Int. Work. on the Next Gen. of Linear Colliders*, SLAC-335, (1989).
2. T. O. Raubenheimer, L. Z. Rivkin, R. D. Ruth, "Damping Ring Designs for a TeV Linear Collider", SLAC-PUB 4868 (1988) and *Proceedings of the DPF Summer Study, Snowmass '88*.
3. L. Z. Rivkin, "Damping Ring for the SLC", Ph.D. Thesis, California Inst. Tech. (1986).
4. L. Z. Rivkin, et al., "Bunch Lengthening in the SLC Damping Ring", SLAC-PUB-4645 (1988).
5. K. Thompson and R. D. Ruth, "Multibunch instabilities in Subsystems of 0.5 and 1.0 TeV Linear Colliders", SLAC-PUB-4800 (1988) and *Proceedings of the DPF Summer Study, Snowmass '88*.
6. M. S. Zisman, S. Chattopadhyay, J. J. Bisognano, "ZAP User's Manual", LBL-21270 (1986).
7. T. O. Raubenheimer and R. D. Ruth, "Analytic Estimates of Coupling in Damping Rings", SLAC-PUB-4914 and presented at this conference.
8. L. Smith, "Effects of Wigglers and Undulators on Beam Dynamics", LBL-21391 (1986) and presented at the *13th Int. Conf. on High Energy Acc.*, Novosibirsk, USSR (1986).
9. K. Halbach, *J. Appl. Phys.*, **57**, 3605 (1985).
10. K. Halbach, private communication.

DISCLAIMER

This report was prepared as an account of work sponsored by an agency of the United States Government. Neither the United States Government nor any agency thereof, nor any of their employees, makes any warranty, express or implied, or assumes any legal liability or responsibility for the accuracy, completeness, or usefulness of any information, apparatus, product, or process disclosed, or represents that its use would not infringe privately owned rights. Reference herein to any specific commercial product, process, or service by trade name, trademark, manufacturer, or otherwise does not necessarily constitute or imply its endorsement, recommendation, or favoring by the United States Government or any agency thereof. The views and opinions of authors expressed herein do not necessarily state or reflect those of the United States Government or any agency thereof.